Direct 3D-printing of microlens on single mode polarization-stable VCSEL chip for miniaturized optical spectroscopy

Qingyue Li, Vincent Raimbault, Pierre-François Calmon, Benjamin Reig, Pierluigi Debernardi, Heidi Ottevaere, Jean Baptiste Doucet, Julien Roul, Véronique Bardinal

JOM Journal of Optical Microsystems

RESEARCH PAPER

Direct 3D-printing of microlens on single mode polarization-stable VCSEL chip for miniaturized optical spectroscopy

Qingyue Li,[a] Vincent Raimbault,[a] Pierre-François Calmon,[a] Benjamin Reig,[a] Pierluigi Debernardi,[b] Heidi Ottevaere,[c] Jean-Baptiste Doucet,[a] Julien Roul,[a] and Véronique Bardinal[a,*]

[a]University of Toulouse, CNRS, LAAS, Toulouse, France
[b]CNR-IEIIT c/o Politecnico di Torino, Torino, Italy
[c]Vrije Universiteit Brussel and Flanders Make, Department of Applied Physics and Photonics, Brussels, Belgium

ABSTRACT. In this work, two-photon polymerization three-dimensional laser writing is used to integrate a microlens on the surface of a single mode polarization-stable vertical-cavity surface-emitting laser (VCSEL) to be used as a current-driven tunable source in a compact optical guided-wave gas sensor. The writing conditions are optimized to enable on-demand room temperature and single-step fabrication at a post-mounting stage. We show that a writing time of 5 min is sufficient to fabricate a microlens that efficiently reduces the VCSEL beam divergence, without significant change on its emitted power or polarization stability. The lens addition reduces the spectral available range at high injection currents. A two-dimensional optical modeling of the gain characteristics is used to explain this effect and a new transverse design is proposed to avoid this issue.

Keywords: VCSEL chip; microlens; beam shaping; two photon three-dimensional direct laser writing; optical microsystems; modal behavior

Paper 23001G received Feb. 7, 2023; revised Jun. 13, 2023; accepted Jun. 29, 2023; published Jul. 13, 2023.

1 Introduction

Due to their high compactness, low power consumption, circular beam emission, and parallel operation capability, near infra-red (NIR) vertical-cavity surface-emitting lasers (VCSELs) have become essential sources for compact sensing systems, such as for three-dimensional (3D)-imaging in smartphones distance ranging, in automotive field, or miniaturized spectroscopy applied to biology or environment.[1] For most of these applications, single-mode (SM) and polarization-stable (PS) laser emission coupled with high power efficiency is required. These features are now well mastered in commercial 850 nm VCSELs sources, for instance by etching a shallow surface subwavelength grating at the device surface and combining this with an appropriate oxide aperture diameter.[2,3] However, similar VCSELs chips having a reduced divergence are not yet commercially available. Beam shaping of these devices is nevertheless crucial because, although smaller than for a LED or an edge-emitting laser diode, their beam diameter becomes too large for most uses as soon as the working distance exceeds a few millimeters. Many works were reported on the hybrid assembly of microoptical elements with VCSELs single device or arrays, but these methods require tricky alignment steps.[4–7] Several monolithic solutions were also

*Address all correspondence to Véronique Bardinal, bardinal@laas.fr

proposed to directly integrate a microlens within the III–V semiconductor device. One can cite for instance recent work on anisotropic wet etching of an aspherical microlens in the first layer of the VCSEL epitaxial structure[8] or dry etching of novel two-dimensional nanoscale metasurfaces.[9] However, these innovative methods may result in an alteration of the electrical properties of the device or are not applicable to lasers operating above 900 nm, i.e., in a spectral range in which the GaAs substrate is transparent. Direct fabrication using low-cost polymer-based technologies remains easier for beam shaping of standard 850 nm VCSELs.[10] In the literature, this approach was mainly developed at the wafer-scale, using standard photolithography in thick photoresists for pedestal fabrication and dispensing techniques for subsequent hemispherical lens deposition on the pedestal surface.[11–13] The authors recently developed an alternative method to enable similar integration on a single small-sized singlemode VCSEL chip. It is based on the use of thick dry resist films and direct UV laser writing.[14] In this work, we exploit the superior advantages of 3D two-photon-polymerization technique to fabricate a similar microlens at a post-mounting stage, but in a single step and with better control of the shape that can perfectly match the aimed design. Lens optical properties are studied as a function of writing parameters. Using optimized conditions, we demonstrate that the beam divergence reduction of an SM-PS VCSEL chip achievable by this technique is as effective as with our previous method, with an unchanged power level and a reduced fabrication time from ~2 days to 5 min. We also investigate the spectral behavior of a lensed device to enable its use as a current-controlled tunable single-mode probe in a microresonator-based optical sensor. We show that the SM emission range is reduced after lens integration and solutions are proposed to address this issue.

2 Requirements on VCSEL Sources for Compact Optical Sensing

The final objective of this work is to develop a compact optical NH_3 gas sensor based on a low-cost polymer microring resonator[15] designed to operate at 850 nm and including a sensitive layer on its surface [Fig. 1(a)]. In the presence of NH_3, the refractive index of this layer varies strongly in the NIR region.[16,17] This leads to a modification of the resonance conditions in the optical microring and a significant change in its transmission spectrum (spectral shift $\Delta\lambda$ and/or peak intensity change ΔP) [Fig. 1(b)]. These optical variations can be detected using a low-cost standard silicon photodiode and related to the gas concentration according to the degree of NH_3 level. The interest of this system lies in a label-free detection based on a reversible reaction at room temperature. It requires, however, the use of a compact NIR single mode source that can be spectrally tunable over a few nanometers, such as a VCSEL.[18] The polarization of the emitted beam must also be stable to ensure optimal coupling to the waveguide through the grating coupler.

A commercial single mode polarization-stable VCSEL die was chosen as the probe source to take advantage of its suitable performances (850 nm/Philips ULM-Photonics).[2] As seen on scanning electron microscopy (SEM) images [Fig. 2(b)], a 150 nm-period one-dimensional (1D) shallow grating is etched at the device surface center over an area of 4.6 μm in diameter.

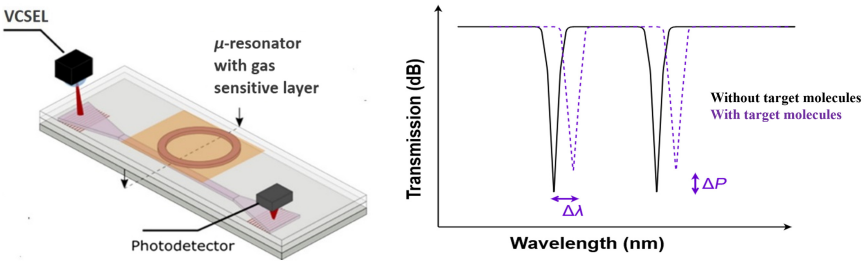

Fig. 1 (a) Schematic view of the final gas sensing microsystem based on low-cost polymer microresonator. (b) Principle of gas detection by measuring the changes in the transmission spectrum of the microresonator using a tunable compact VCSEL.

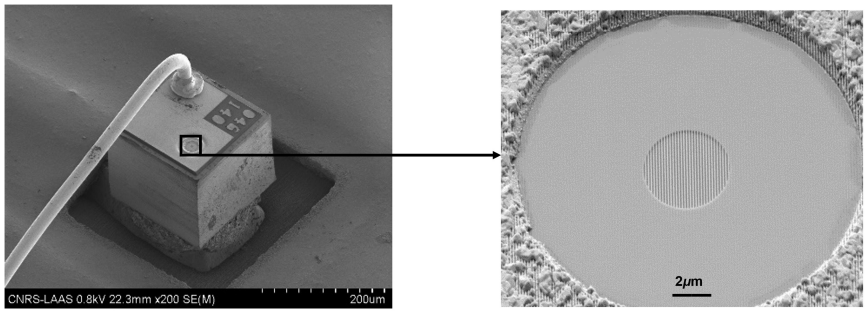

Fig. 2 (a) SEM views of an SM-PS VCSEL chip mounted and wired on a PCB. (b) Zoom on the emitting surface on top of which a shallow 1D grating is etched for polarization control.

Due to this optical design, the laser emits in a stable linear polarization regime (degree of polarization DOP > 80%). Moreover, a side-mode suppression ratio (SMSR) of more than 10 dB is observed for applied current up to 9 mA (see Fig. 3). As a result, the laser peak can be tuned continuously with no mode hopping over a spectral range of ~7 nm. This single mode tuning range is suitable for probing at least two peaks in the transmission spectrum of the microresonator during gas detection.

The beam divergence of this SM-PS VCSEL was measured using a beam profiler camera. Its value was 14.4°@3 mA (full angle at $1/e^2$), which means the beam diameter at a distance of 2 mm was much larger (>0.25 mm) than the size of the light coupling area of the sensor (fixed to 100×100 μm^2 to ensure a small footprint of the optical microsystem). The challenge relies, therefore, in the integration of a collimating microlens using a fabrication method applicable at a post mounting/assembly stage to a small-sized chip (200 $\mu m \times 200$ $\mu m \times 150$ μm) [Fig. 2(a)].

As above-mentioned, a first method was successfully developed by the authors to reduce the beam divergence of similar chips to ~3 deg (full angle at $1/e^2$). This method required, however, three successive fabrication steps: (i) soft-thermal printing of several dry resist films, (ii) UV direct laser writing of a cylindrical pedestal, and (iii) inkjet printing of droplet to form a hemispherical lens on the pedestal surface.[13,14] With this method, only discrete values of pedestal heights and ink droplets numbers could be chosen. Here, we develop a more straightforward and flexible method based on two-photon polymerization (2PP) 3D-printing.

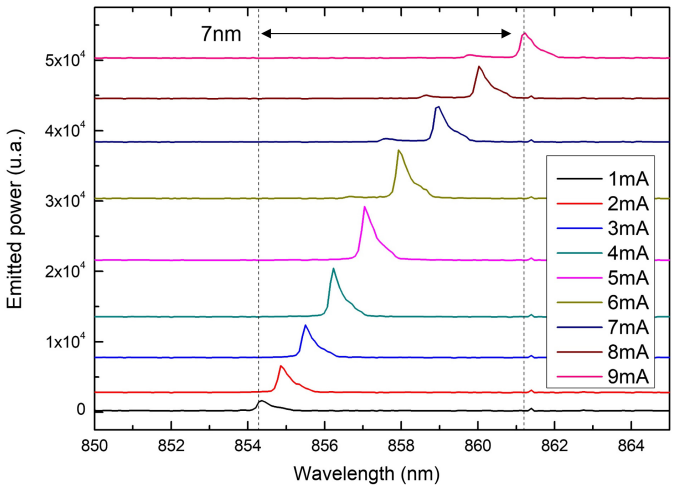

Fig. 3 Measurement of the emitted spectrum of the VCSEL chip as a function of applied current. Single-mode emission can be tuned over 7 nm with no mode hopping.

3 On-Demand Fabrication on Chip Using Free-Form 3D Printing

3.1 Two-Photon Polymerization Direct-Laser Writing

In recent years, additive manufacturing (3D printing) has proved to be a viable alternative to conventional planar fabrication technologies, with applications in photonics, biology, or lab-on-chip among others. 3D printing offers indeed more degrees of freedom on shapes that can be achieved, enabling new fabrication schemes. As a non-collective method, 3D printing is well suited to fabricate single objects, which is typically the case when creating a microlens on top of a single VCSEL chip. Compared with other additive manufacturing technologies, 2PP 3D printing attracts more and more attention in micro-optics field, as it enables the fabrication of freeform optical elements with high resolution (<0.2 μm) and high accuracy ($< \pm 0.5\%$). Considering the precision required for the fabrication of micro-optical elements, this technique offers appropriate characteristics[19–21] and was successfully applied to fabricate a complete miniature visible spectrometer,[22] as well as for the precise fabrication of micro-optical elements on single-mode optical fibers[23] or LED devices.[24] It was also recently exploited to couple VCSEL arrays to multimode fibers for data transmission experiments[25] and to fabricate an external collimator for VCSEL used in 3D sensing systems.[26] However, direct fabrication on a VCSEL chip to be used for miniaturized optical spectroscopy has not been yet reported.

The 2PP writing principle used is shown in Fig. 4. The photosensitive material is polymerized by absorption of two photons simultaneously. This non-linear optical process occurs when an ultrashort pulse laser is focused tightly in a small area. The size of this voxel is related to the laser spot, the laser power, and the properties of the material itself. By scanning the laser beam throughout the material or by moving the sample with a fixed laser spot, a 3D structure can be polymerized. As shown in Fig. 4(a), the substrate is immersed into the photosensitive liquid resist. In our case, the substrate is a printed circuit board (PCB) with a mounted VCSEL chip. By slowly moving the sample up, the polymerization occurs layer by layer at the computed positions. Once the exposure is complete, a development solution is used to remove the uncured resist. The set-up used is photonic professional L-3D (Nanoscribe Gmbh) with a 780 nm femtosecond laser source (pulse $\approx$ 100 fs; repetition rate = 80 MHz) and a writing intensity ranging from 0.982 to 1.547 TW/cm^2 depending on the chosen exposure power.[27] In order to obtain a good compromise in terms of resolution and writing time, a 63× objective was selected and used in dip-in laser lithography mode suited for high-resolution patterning on a non-transparent substrate. The 63× microscope objective has a numerical aperture (NA) of 1.4, giving a working distance of 190 μm. This configuration leads to a voxel size of 160 nm in X/Y axes and about 700 nm in the Z axis. The chosen photoresist was IP-Dip resist, as it is well suited to the fabrication of high resolution/high aspect-ratios optical elements with a high refractive index in the near-infrared spectral range.

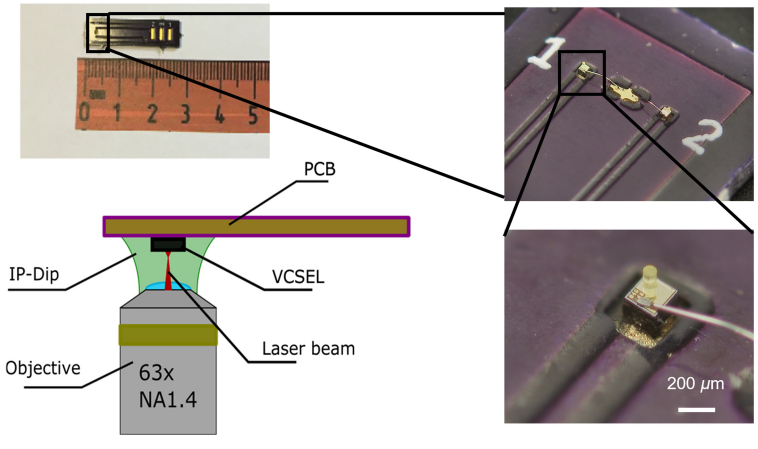

Fig. 4 (a) Principle of the two-photon polymerization 3D printing on VCSEL chip (Nanoscribe Gmbh). The VCSEL mounted onto a PCB is dipped into the photoresist, which is in direct contact with the objective lens. (b) Zoom on a lensed-VCSEL chip mounted on the PCB.

3.2 Microlens Design

ZEMAX optical modeling software was used to design a micro-optical element made of a cylindrical polymer pedestal surmounted by a hemispherical lens for collimating the VCSEL beam (Fig. 5). We used the ZEMAX merit function with GBPD operand to minimize the Gaussian beam paraxial divergence taking into account the optical properties of the lens material[28,29] and the possible ranges for lens dimensions, namely diameter D, sag T, and pedestal height L, which are limited by technological constraints. Since the emitting area is non-centered on the VCSEL chip [Fig. 6(a)], the lens diameter D cannot be chosen larger than 80 μm. For 80 μm, the

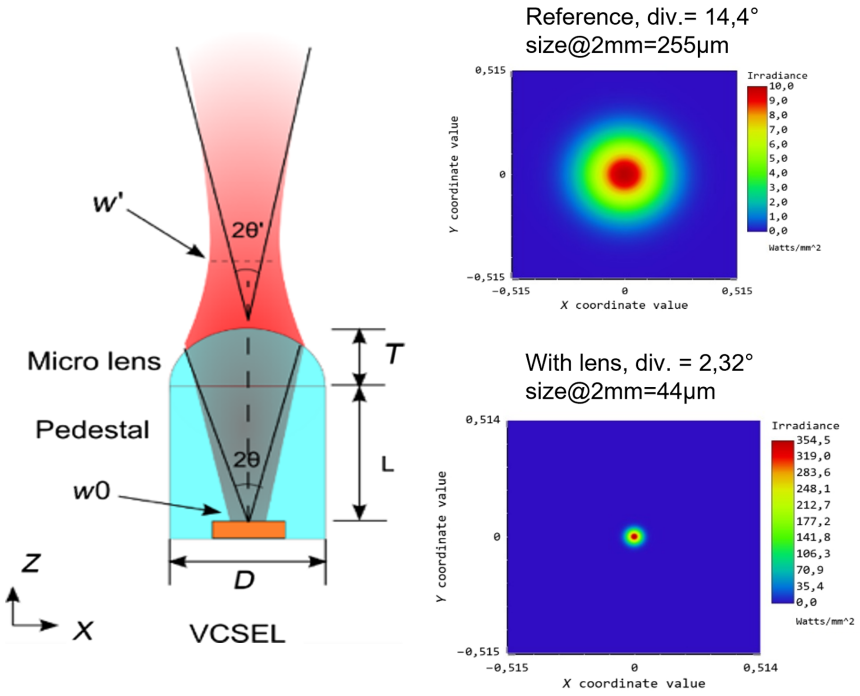

Fig. 5 (a) Lens design. (b) Spatial distribution of the beam irradiance calculated using ZEMAX (Gaussian beam propagation) at a distance of 2 mm for the reference without lens (top) and with lens (bottom). The corresponding theoretical divergence is reduced from 14.4 deg to 2.32 deg (full angle at $1/e^2$).

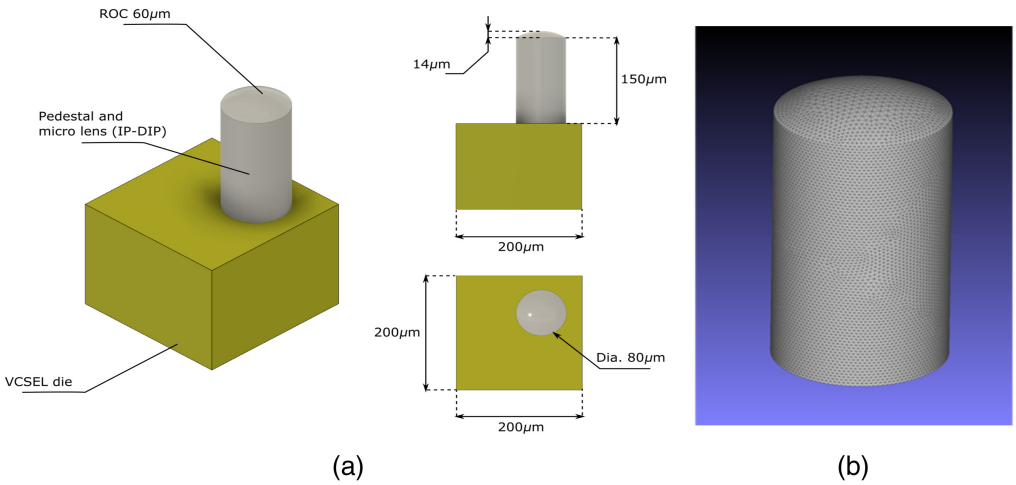

Fig. 6 (a) 3D CAD design of the pedestal + lens system to be fabricated on the VCSEL die. (b) Corresponding STL mesh comprising 22,284 faces and 11,414 vertices.

divergence can be theoretically reduced from 14.4 deg to 2.32 deg with a 150 μm-thick pedestal, a lens sag of 14 μm and a radius of curvature (ROC) of 60 μm. This corresponds to a beam size of less than 50 μm at 2 mm from the lens output surface, which fits well our sensor requirements. Note that this divergence value could be further reduced, for example, by increasing the pedestal height L. However, it is preferable to limit this parameter to 150μm to maintain a reasonable aspect ratio for the entire micro-optical element ($\leq$1 : 2).

3.3 3D Printing Optimization

Owing to the nature of 2PP technology, the pedestal and the micro lens can be designed as a single unit, with the additional benefit of being able to arbitrarily change all dimensions. This design can be done using a conventional 3D computer-aided-design (CAD) software. In our case, we used FreeCAD, an open-source parametric 3D CAD software. The resulting design is then exported as a.STL file, which is a file format commonly used for 3D printing. While the native parametric 3D CAD design is composed of primitives (i.e., a combination of solids such as cubes, cylinders, spheres...), the STL file is an approximated version of the parametric design that uses triangular planes to reproduce the surface geometry of the 3D model. The Nanoscribe set-up uses STL file format as an input, as such the settings for exporting the 3D parametric design to an STL file are critical: coarse settings would lead to large facets and would be detrimental to the overall print quality, whereas very refined parameter would lead to enormous files and much longer processing while not bringing additional benefits to the print quality. Our settings are a compromise between file size and print quality. An illustration of STL file for the pedestal and microlens is shown in Fig. 6.

As mentioned above, the optimal writing conditions result from a compromise between time and resolution. We tried several combinations of 100% exposure power with scan speeds of 30 and 50 mm/s, and 40% to 63% exposure powers with scan speeds of 10 and 30 mm/s to optimize lens shape and morphology while keeping a maximal fabrication time of 1 h per lens. SEM images of final 3D lenses optimized for three different slicing resolutions (SR) are shown in Fig. 7(b). As expected, the surface of a lens fabricated by 3D-printing is less smooth than that fabricated with a non-contact dispensing method such as inkjet printing [Fig. 7(a)]. Layered patterns are visible, especially for large SR. However, the geometry of the pedestal and of the lens can be better adjusted and controlled with this method.

3.4 Lens Properties

Lens dimensions were measured using white-light optical profilometry (Bruker Contour GTI and S neox from Sensofar) [see typical images in Fig. 8(b)]. After a calibration step to compensate for the material shrinkage that occurs during 3D-printing (typically ~4% depending on the

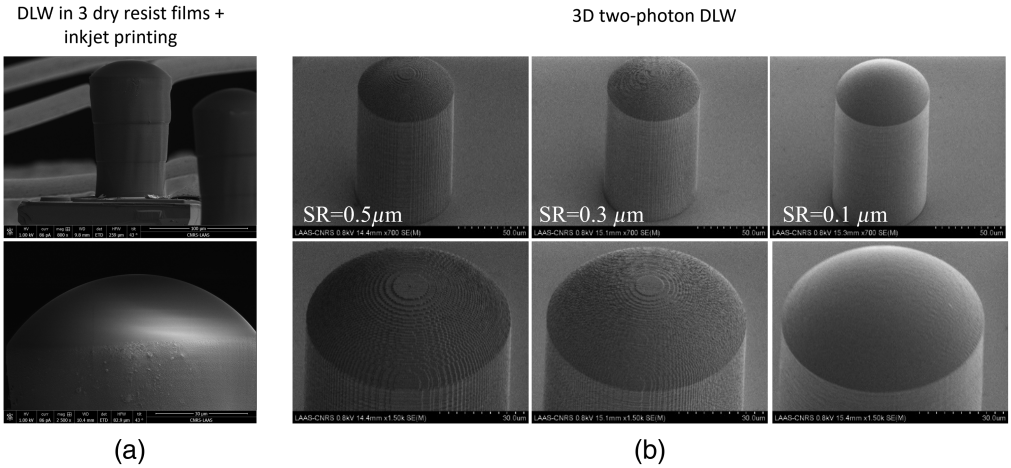

Fig. 7 SEM views of a microlens fabricated (a) by our former technique (successive soft-printing of three dry resist films + DLW+ inkjet printing), (b) by 3D-printing using three different SRs (SR = 0.5, 0.3, and 0.1 μm) with scanning speeds of 30, 30, and 50 mm/s, and exposure powers of 63%, 50%, and 40%, respectively (maximal intensity for 63%: 1.547 TW/cm^2).

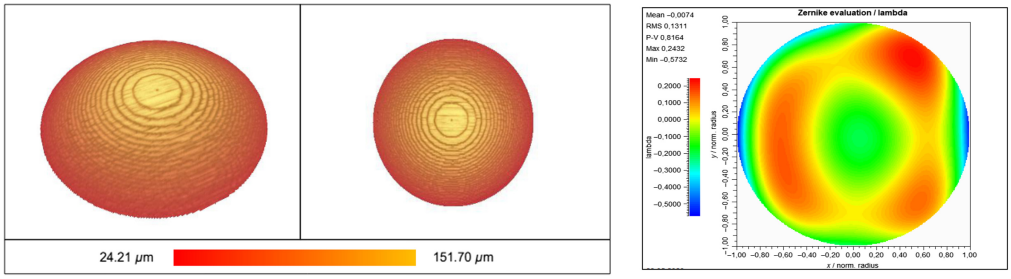

(a) (b)

Fig. 8 (a) 3D and 2D images of a lens printed with an SR of 0.3 μm acquired with a S neox optical profilometer. (b) Example of a plot acquired by Mach–Zehnder interferometry used to calculate the focal length and the RMS aberrations (before calibration).

exposure power), the final lens diameter and sag were measured at $D = 78.78 \pm 1.67$ μm and $T = 13.66 \pm 0.93$ μm, respectively, in good agreement with the desired values. The ROC measured for three different SR is shown in Fig. 9(a). As seen, the dispersion of the values increases for lower resolutions. Nevertheless, we measured for the least favorable resolution (SR $= 0.5$ μm) a ROC equal to 60.36 ± 1.67 μm, which is also in good agreement with expectations.

Lens surface roughness was also characterized using optical profilometry. These measurements confirmed the SEM observations: the lower the slicing value, the lower the roughness [Fig. 9(b)]. The minimal value was indeed obtained for 0.1 μm, with a root means square height S_q of 81.65 nm, of the same order of magnitude as that reported for standard 2PP-DLW techniques[30] However, in this case, the total writing time is 60 min, whereas it is much shorter for lower resolutions: 10 min and 5 min, for 0.3 and 0.5 μm, respectively. Given the moderate difference in surface roughness observed between the 0.3 and 0.5 μm cases (98 versus 88 nm) and the significant gain in fabrication time (×2), the SR used for lens fabrication on the VCSEL chip was finally set at 0.5 μm.

In addition, a lens array printed on a glass substrate using the average resolution (SR $= 0.3$ μm) was characterized using a Mach–Zehnder interferometer. With this set-up, it was possible to determine the focal length through the interpretation of the observed fringe pattern[31] [see example for one lens in Fig. 8(b)]. A mean value of 98.6 ± 2.3 μm was determined (six lenses measured). The numerical aperture of the lens (NA $= 0.35 \pm 0.02$) and the optical aberrations (RMS $= 0.143 \pm 0.04$ lambda) were also derived from these measurements. The latter value is higher than $\lambda/14$, indicating that the lenses are not diffraction-limited. However, their quality seems sufficient for our non-imaging application. Additional measurements for the other resolutions are still in progress.

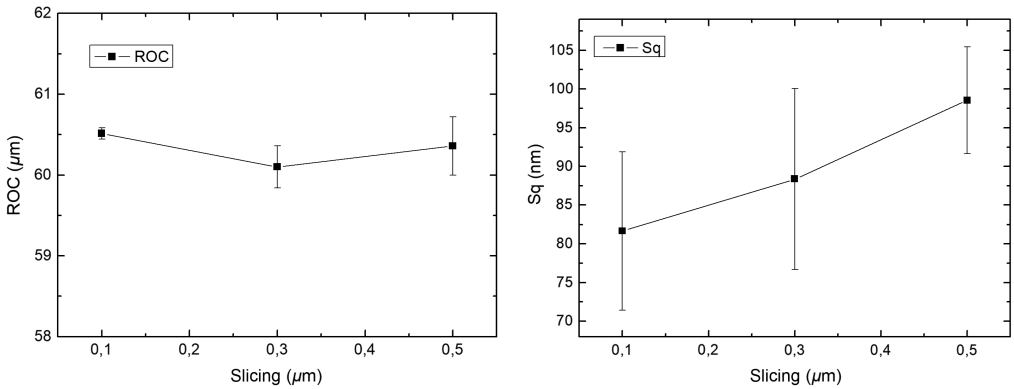

(a) (b)

Fig. 9 (a) ROC and (b) surface roughness Sq (root mean square height).

4 Application to VCSEL Chip Collimation

As mentioned above, a coarse resolution of 0.5 μm was selected for the rest of the study in order to obtain a short writing time with a limited effect on the lens optical quality. We applied this process to single VCSEL chips at a post mounting stage, i.e., on single chips already mounted on a PCB [Fig. 10(a)] and also at a post-assembly stage, i.e., on already wired chips [Fig. 10(b)]. As seen, lenses were in both cases well positioned relatively to the emission area.

4.1 Beam Divergence and Emitted Power

After lens fabrication, the profile of the VCSEL Gaussian beam was acquired for two different axial positions with a beam profiler camera placed on a moving stage. By transforming the measured intensity profiles using a Gaussian fit to extract the waist sizes at both positions and knowing the distance between them, the corresponding beam divergence could be determined and found to be 3.0 ± 0.1 deg (full angle at $1/e^2$) [Fig. 11(a)]. This value is comparable to the one previously obtained by the authors using UV direct laser writing in dry films coupled to inkjet dispense. It is higher than the theoretical value given by the model (2.32 deg). A better fit with the experimental value is found by taking into account in the model the fabrication uncertainties on lens dimensions and most importantly, by assuming that the initial beam waist is not located at the VCSEL surface but 3 μm beneath it (i.e., at the position of the quantum well active zone in the laser). This indicates that the lens design could be further optimized with the model and that a minimal divergence of 2.5 deg is experimentally achievable. Nevertheless, the spot size is estimated to be 55 μm at a distance of 2 mm (instead of 44 μm expected), which is sufficiently for the aimed application. Concerning the VCSEL optoelectronic behavior after lens integration, a slight modification of the threshold current is visible on the light-current curve. This is due to the change in the reflectance of the top mirror, linked to the presence of the IP-Dip lens polymer

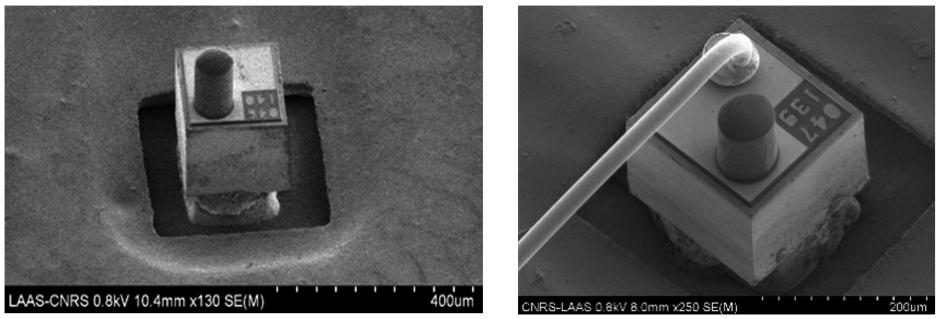

(a) (b)

Fig. 10 SEM views of a lensed VCSEL chip mounted on a PCB. Lens fabrication can be applied (a) before or (b) after wire bonding.

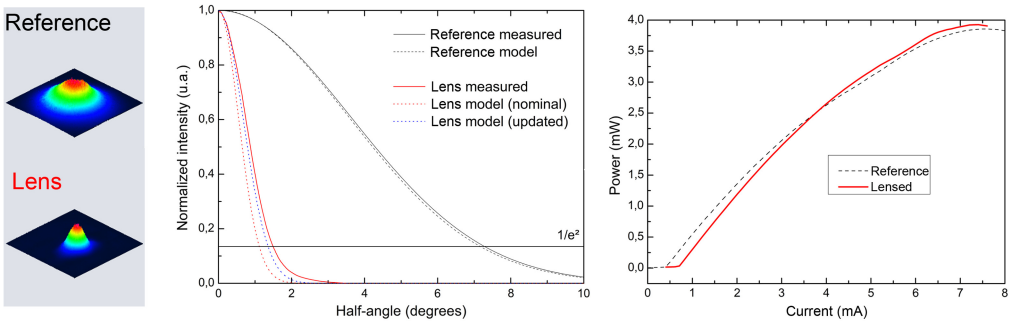

(a) (b)

Fig. 11 (a) Comparison of the normalized angular beam distributions of the reference and lensed VCSEL chips (solid lines: experimental, dotted lines: model). (b) Light–current curve measured for both devices.

material at the VCSEL surface. The output emitted power level is, however, found to be similar to that of the reference device, showing no significant effect despite lower surface quality [Fig. 11(b)]. We also checked that the degree of polarization of the emitted beam was kept higher than 75%, which means the grating effect on polarization selection was preserved after lens integration.

4.2 Available Tuning Range Under Current Variation

The evolution of the emission spectrum as a function of the applied current was also measured after lens integration (Fig. 12). The SMSR remained higher than 10 dB for injection currents below 5 mA, but a dual mode emission progressively appeared for upper currents. This led to a final single mode tuning range of only ~3 nm. This behavior can be attributed to the fact that the respective diameters of the polarization grating (4 μm) and of the buried oxide aperture (6 μm) of the used VCSEL chip are suited to achieve a single-mode operation with an output medium in the air and not in a polymer material.

To get a better understanding of this behavior, we performed optical simulations of threshold gain features in a VCSEL device with and without lens insertion (Fig. 13).[32] For both cases, the calculated fundamental mode threshold gain as a function of internal maximum temperature is

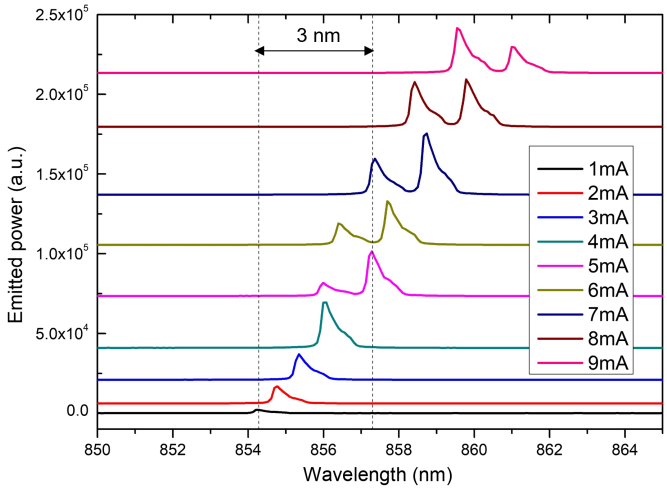

Fig. 12 Emitted spectrum of the VCSEL chip after lens integration as a function of applied current. The tuning range with SM emission (SMSR > 10 dB) is reduced to ~3 nm.

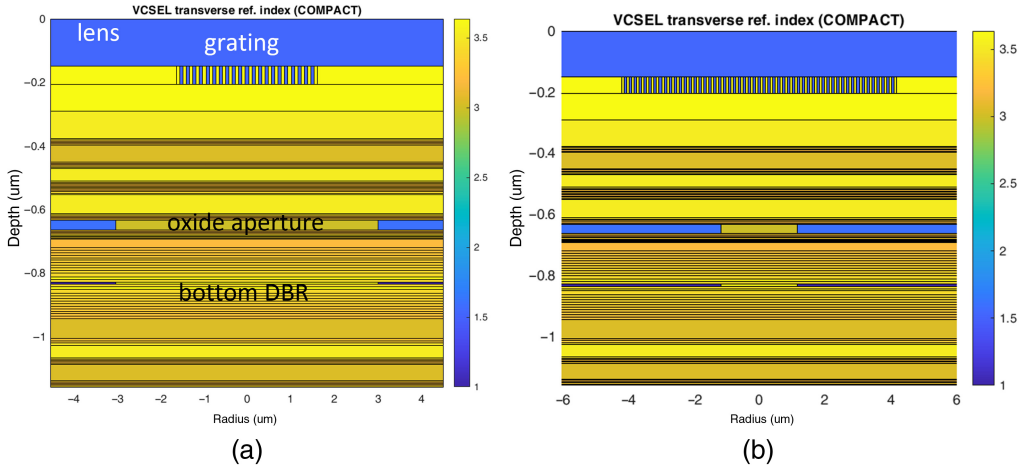

Fig. 13 Compressed index cross section map (without repetitions) of the lensed-VCSEL structure (a) (diameter of grating relief: 4 μm, diameter of oxide aperture: 6 μm) and (b) new proposed design (grating relief: 8 μm, oxide aperture: 2.2 μm).

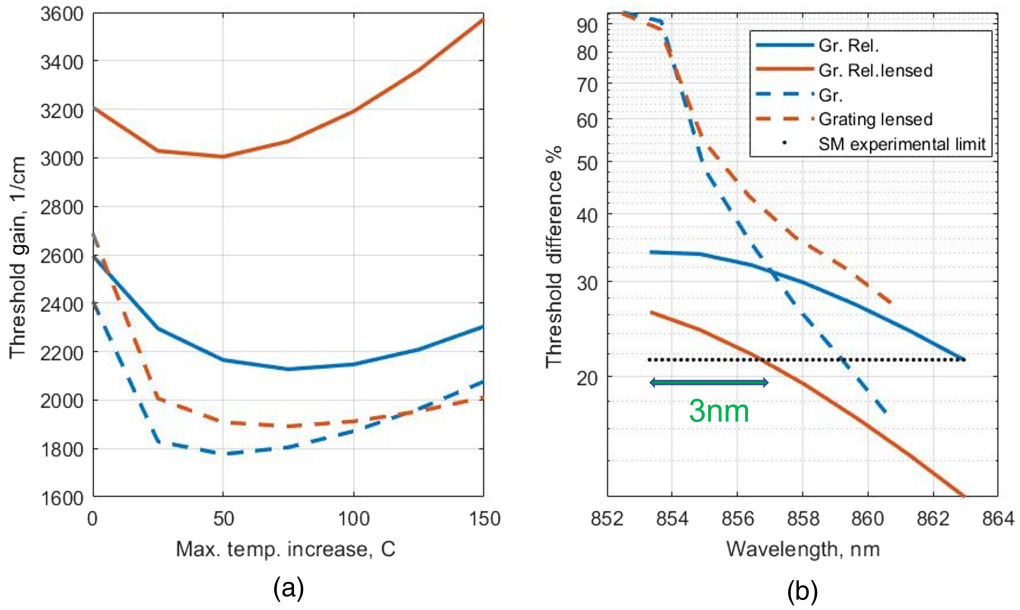

Fig. 14 (a) Calculated fundamental threshold gain G_0 for the reference (blue) and the lensed (red) device (solid lines) and new design (dashed lines) as a function of the temperature increase. (b) Corresponding modal gain difference $(1 - G_0/G_1) \times 100$.

plotted in Fig. 14(a). The corresponding difference between the fundamental mode gain (G_0) and the second transverse mode gain (G_1) is defined as: $(1 - G_0/G_1) \times 100$ and shown in Fig. 14(b). The reference device stays single mode over all the current range (blue solid curve), as measured. An internal spatial temperature profile with a peak of 150°C at the cavity section is needed to match the experimental wavelength variation, by assuming the standard temperature dependence of the refractive indices ($2.3\ 10^{-4}$).[33,34] The thermal lensing diminishes the gain difference, which reaches an estimated value of 21% for the lens-less device at the internal temperature increase of 150°C. Integrating the lens, the gain threshold G_0 increases by 20% [see red solid curve in Fig. 14(a)], and the gain difference between the two modes diminishes. This is caused by the lower index step between the VCSEL facet and the polymer lens. Assuming for SM operation the computed value of 21%, we get for the lensed VCSEL an SM range of 3 nm, which is determined by the continuous red curve crossing the 21% gain difference (dotted line), as shown by the green arrow in Fig. 14(b). This value corresponds to the experimental observations.

Although this reduced SM tuning range is still exploitable for our sensor provided a suitable design of the optical resonator with a free spectral range of less than 3 nm, it would be preferable to relax the technological constraints on the microring fabrication and keep the entire initial spectral tuning range available. A first possibility would be to restore the original index step at the VCSEL facet, by inserting an air gap between the VCSEL surface and the cylindrical lens, which would imply a suspended lens with external pillars. The fabrication of such a 3D microstructure is feasible using 2PP photopolymerization. ZEMAX optical modeling indicates that a beam collimation as efficient as with a standard lens on a bulk pedestal could be obtained in this case by simply choosing a smaller ROC. However, this approach would require the creation of an air gap with a thickness of at least few microns between the VCSEL and the lens bottom surface, to ensure an efficient removal of un-polymerized material after fabrication. This large air gap might render the lens mechanically more fragile compared to a bulk lens. A simpler way would consist instead in slightly modifying the VCSEL design without changing the epilayer nor the parameters of the grating that serve to fix the polarization. Namely, it would consist in a singlemode VCSEL not based on the surface relief technique, but rather on small oxide aperture with a transverse design suited for the aimed application. As shown in Fig. 14(b), by simply choosing a reduced oxide aperture size of 2.2 μm and a polarization grating area with a much larger diameter (8 μm), the latter can be regarded as infinite for the optical field. Our modeling results show that this device provides better threshold performances and polarization-stable single mode operation over the whole tuning range, as desired.

5 Conclusions

To conclude, the collimation of a single mode and polarization-stable VCSEL chip to be used as a spectrally tunable probe in a miniaturized sensor was performed using two-photon polymerization laser printing (2PP-DLW) technique. The conditions of lens fabrication were optimized on test substrates considering three different SR (0.1/0.3/0.5 μm). Surface roughness Sq was measured by white light optical profilometry and found comprised between 81 nm RMS (SR = 0.1 μm) and 98 nm RMS (SR = 0.5 μm). Mach–Zehnder interferometry was also exploited to check the focal length value (98 μm) and the optical aberrations (0.18 lambda RMS) for the middle resolution (SR = 0.3 μm). Finally, one-step integration of a 3D lens on the surface of a VCSEL chip was achieved using the lowest resolution tested (SR = 0.5 μm) leading to a processing time of 5 min. After lens fabrication, the device beam divergence was reduced from 14.4 deg to 3.0 deg (full angle at $1/e^2$) without significant loss in the emitted power. These results are comparable to those obtained in a previous work that involved three different fabrication methods (dry films soft-printing, UV direct laser writing, and inkjet printing) and long thermal steps. This demonstrates the superior advantage of 2PP 3D printing as a fast and accurate technique for VCSEL chip collimation at a post-mounting stage. Comparison between experiments and modelling showed a satisfactory agreement by taking into account the fabrication uncertainties and by assuming in the model a position of the beam waist 3 μm beneath the VCSEL's output surface. Finally, the study of the spectral behavior of a lensed VCSEL submitted to electrical current variation was also studied. After lens integration, a reduction from 7 to 3 nm in the available single-mode spectral range was observed. We explained this behavior by computing the optical transverse mode losses and we proposed a specific design based on the same VCSEL wafer layout to extend the available single-mode tuning range and additionally improve the threshold conditions. Future work will consist of exploring this approach and exploit the final device in optical gas sensing experiments. Interferometry measurements will be also continued and the integration of aspherical and/or suspended lens on VCSEL chip will be considered to further exploit the specific advantages of 3D femtosecond laser printing.

Data Availability Statement

The data that support the findings of this study are available from the corresponding author, VB, upon reasonable request.

Acknowledgments

This work was supported by Agence Nationale de la Recherche (ANR) (Gant No. ANR-15-CE19-0012 DOCT-VCSEL). The authors gratefully acknowledge Philipp Gerlach, who was working for Philips Ulm Photonics when contributing to this work and now with pmdindustrial gmbH and Pr. Philippe Menini and Pr. Thierry Camps from LAAS-CNRS for fruitful discussions. This work was supported by LAAS-CNRS micro and nanotechnologies platform, a member of the RENATECH French national network. This research was also supported by the Methusalem and Hercules foundations and the OZR of the Vrije Universiteit Brussel (VUB).

References

1. M. Dummer et al., "The role of VCSELs in 3D sensing and LiDAR," *Proc. SPIE* **11692**, 116920C (2021).
2. M. A. Verschuuren et al., "Improved performance of polarization-stable VCSELs by monolithic sub-wavelength gratings produced by soft nano-imprint lithography," *Nanotechnology* **22**(50), 505201 (2011).
3. P. Debernardi, J. M. Ostermann, and R. Michalzik, "VCSEL polarization control by monolithic surface gratings: a survey of modelling and experimental activities," *Proc. SPIE* **7009**, 700903 (2008).
4. H. L. Chen et al., "Collimating diode laser beams from a large area VCSEL-array using microlens array," *IEEE Photonics Technol. Lett.* **11**(5), 506–508 (1999).
5. G. Kim, X. Han, and R. T. Chen, "Crosstalk and interconnection distance considerations for board-to-board optical interconnects using 2-D VCSEL and microlens array," *IEEE Photonics Technol. Lett.* **12**(6), 743–745 (2000).
6. A. Tuantranont et al., "Optical beam steering using MEMS-controllable microlens array," *Sens. Actuators A: Phys.* **91**(3), 363–372 (2001).

7. C. Vergnenègre et al., "Integrated optical detection subsystem for functional genomic analysis biosensor," *Proc. SPIE* **5969**, 596912 (2005).
8. Y. Huang et al., "Monolithic microlens VCSELs with high beam quality," *IEEE Photonics J.* **9**, 1504408 (2017).
9. Y.-Y. Xie et al., "Metasurface-integrated vertical cavity surface-emitting lasers for programmable directional lasing emissions," *Nat. Nanotechnol.* **15**, 125–130 (2020).
10. V. Bardinal et al., "Collective microoptics technologies for VCSEL photonic integration," *Adv. Opt. Technol.* **2011**, 1–11 (2011).
11. W. C. Chen et al., "Fabrication of inkjet-printed SU-8 photoresist microlenses using hydrophilic confinement," *J. Micromech. Microeng.* **23**, 065008 (2013).
12. V. Bardinal et al., "Spotted custom lenses to tailor the divergence of vertical-cavity surface-emitting lasers," *IEEE Photonics Technol. Lett.* **22**, 1592–1594 (2010).
13. S. L. Tan et al., "High pulsed power VCSEL arrays with polymer microlenses formed by photoacid diffusion," *Opt. Express* **28**, 20095–20105 (2020).
14. Y. Zhao et al., "Implementation of integrated VCSEL-based optical feedback interferometry microfluidic sensor system with polymer microoptics," *Appl. Sci.* **9**(24), 5484 (2019).
15. M. D. Garcia et al., "An analytical approach to predict maximal sensitivity of microring resonators for absorption spectroscopy," *J. Lightwave Technol.* **37**(21), 5500–5506 (2019).
16. S. Christie et al., "Remote detection of gaseous ammonia using the near infrared transmission properties of polyaniline," *Sens. Actuators B: Chem.* **90**(1-3), 163–169 (2003).
17. A. Airoudj et al., "Integrated SU-8 photonic gas sensors based on PANI polymer devices: comparison between metrological parameters," *Opt. Commun.* **282**(19), 3839–3845 (2009).
18. C. J. Chang-Hasnain et al., "Continuous wavelength tuning of two-electrode vertical cavity surface emitting lasers," *Electron. Lett.* **27**(11), 1002–1003 (1991).
19. K. Sugioka and Y. Cheng, "Femtosecond laser three-dimensional micro- and nanofabrication," *Appl. Phys. Rev.* **1**, 041303 (2014).
20. P. Dietrich et al., "In situ 3D nanoprinting of free-form coupling elements for hybrid photonic integration," *Nat. Photonics* **12**, 241–247 (2018).
21. D. Gonzalez-Hernandez et al., "Micro-optics 3D printed via multi-photon laser lithography," *Adv. Opt. Mater.* **11**, 2201701 (2023).
22. A. Toulouse et al., "3D-printed miniature spectrometer for the visible range with a 100×100 μm^2 footprint," *Light Adv. Manuf.* **2**(1), 20–30 (2021).
23. T. Gissibl et al., "Sub-micrometre accurate free-form optics by three-dimensional printing on single-mode fibres," *Nat. Commun.* **7**(1), 11763 (2016).
24. S. Thiele et al., "Ultra-compact on-chip LED collimation optics by 3D femtosecond direct laser writing," *Opt. Lett.* **41**(13), 3029–3032 (2016).
25. P. Maier et al., "3D-printed facet-attached optical elements for connecting VCSEL and photodiodes to fiber arrays and multi-core fibers," *Opt. Express* **30**, 46602–46625 (2022).
26. B. Chen et al., "Generation of a high-resolution 3D-printed freeform collimator for VCSEL-based 3D-depth sensing," *Opt. Lett.* **45**, 5583–5586 (2020).
27. E. Skliutas et al., "Polymerization mechanisms initiated by spatio-temporally confined light," *Nanophotonics* **10**(4), 1211–1242 (2021).
28. S. Dottermusch et al., "Exposure-dependent refractive index of nanoscribe IP-Dip photoresist layers," *Opt. Lett.* **44**(1), 29–32 (2019).
29. Y. Li et al., "UV to NIR optical properties of IP-Dip, IP-L, and IP-S after two-photon polymerization determined by spectroscopic ellipsometry," *Opt. Mater. Express* **9**, 4318–4328 (2019).
30. K. Vanmol et al., "Two-photon polymerization-based direct laser writing and characterization of microlenses for optical interconnect applications," in *26th Microopt. Conf. (MOC)*, Hamamatsu, Japan, pp. 1–2 (2021).
31. H. Ottevaere and H. Thienpont, "Refractive optical microlenses: an introduction to nomenclature and characterization techniques," in *Encyclopedia of Modern Optics*, Vol. **4**, pp. 21–43, R. D. Guenther, D. G. Steel, and L. Bayvel, eds., Elsevier, Oxford (2004).
32. P. Debernardi and G. P. Bava, "Coupled mode theory: a powerful tool for analyzing complex VCSELs and designing advanced device features," *IEEE J. Sel. Top. Quantum Electron.* **9**(3), 905–917 (2003).
33. A. Tibaldi et al., "VENUS: a vertical-cavity surface-emitting laser electro-opto-thermal NUmerical simulator," *IEEE J. Sel. Top. Quantum Electron.* **25**(6), 1–12 (2019).
34. P. Debernardi et al., "Anisotropic transverse confinement design for electrically pumped 850 nm VCSELs tuned by an intra cavity liquid-crystal cell," *IEEE J. Sel. Top. Quantum Electron.* **28**(1), 1–11 (2022).

Pierre-François Calmon graduated in physics at the Conservatoire National des Arts et Métiers of Paris, France, in 1998. Since 2001, he is a research engineer at LAAS-CNRS clean room

facility and specialist of 2D and 3D laser lithography techniques. He is developing micro and nano technology processes by using bi-photons technique to fabricate micro-optics components.

Benjamin Reig received his MSc degree in micro and nano-systems from Toulouse University, France, in 2008 and his PhD in optoelectronics in 2011. Since 2012, he is a research engineer in LAAS-CNRS clean room facility. His main interest concern materials and devices characterization using microscopy, chemical analysis systems and optical measurements. He is also involved in research on polymer MOEMS and new approaches using FIB technique (focused ions beam) to pattern polymer micro-optics on VCSELs.

Pierluigi Debernardi received the degree in electronics engineering from Politecnico di Torino, Turin, Italy, in 1987. Since 1989, he has been with the Italian National Council of Research. His interests are mainly in the field of the modeling of semiconductor materials and devices for optoelectronic applications. He is currently involved in modeling and designing VCSEL structures with non-circular and/or complex geometries, so as to achieve new and specific performances.

Heidi Ottevaere is a full professor at the Faculty of Engineering of the VUB since October 2009. Since 2019, she chairs the Applied Physics and Photonics Department (TONA) of the Faculty of Engineering that is responsible for the photonics education curriculum at Vrije Universiteit Brussel. She is responsible for the instrumentation and metrology platform at the Photonics Innovation Center and for the biophotonics research unit of the Brussels Photonics Team B-PHOT.

Jean-Baptiste Doucet is a chemistry and technology engineer in LAAS-CNRS clean room facility. He is in charge of 850 nm VCSEL and III-V related devices technology. He is also a specialist of new micro/nano lithography techniques such as Soft Thermal Nanoimprint for nanograting fabrication. His research interest concerns new fabrication methods for VCSEL beam shaping and VCSEL spectral tuning.

Véronique Bardinal graduated in physics at the Institut National des Sciences Appliquées of Toulouse, France, in 1992. She obtained her PhD in optoelectronics in 1995. From 1996 to 1997, she was a research assistant at EPFL, Switzerland. She joined LAAS-CNRS (research unit of French National Scientific Research Center) in 1997. Her research interests include design, epitaxial growth, fabrication and characterization of VCSEL devices, polymer microoptics and more recently liquid crystal-based tunable devices.

Biographies of the other authors are not available.